Buckling behavior of spiral stiffened sandwich FGM cylindrical shells with porous core under axial compression using the FSDT

Nguyen Hoang Quan[1], Vu Minh Duc[2], Nguyen Thi Phuong[2], Le Ngoc Ly[2,*], Nguyen Thi My Trang[2]

[1]University of Transport and Communications, Hanoi 100000, Vietnam
[2]University of Transport Technology, Hanoi 100000, Vietnam

Abstract: The linear buckling behavior of functionally graded cylindrical shells with porous core stiffened by spiral stiffeners under axial compression using the first-order shear deformation theory is presented in this paper. The improved Lekhnitskii's smeared stiffeners technique is applied for shear deformable spiral FGM stiffeners. Approximate analytical solutions are assumed to satisfy the simply supported boundary conditions and the adjacent equilibrium criterion is applied to obtain closed-form relations of buckling loads. Effects of the number of FGM stiffeners, stiffener angle, volume fraction index and porosity coefficient on the buckling behavior of shells are numerically investigated.

Keywords: Functionally graded material; Porous core; Spiral stiffener; Linear buckling; Axial compression; Cylindrical shell; First-order shear deformation theory

1. Introduction

The cylindrical shell is a complex shell structure that is widely applied in engineering throughout the world. Recently, many authors have focused on the buckling behavior of these structures made by advanced composite materials. Porous materials such as metal foams are lightweight materials with excellent energy-absorbing capability and they have received wide application in engineering for plates and shells.

The linear and nonlinear buckling behavior of cylindrical shells made by functionally graded material (FGM) subjected to many load types were investigated by many authors in the world [1-3]. Recently, by using the classical thin shell theory, the nonlinear buckling behavior of FGM cylindrical shells with and without porous core stiffened by orthogonal and spiral stiffeners has been focused

on by using the improved smeared stiffener technique [4-8]. With the same shell theory, the nonlinear buckling behavior of graphene platelet reinforced cylindrical shells stiffened by spiral stiffeners were investigated by Hoa et al. [9]. The effects of porosity on buckling behavior of saturated porous FGM toroidal shell segments were investigated by Babaei et al. [10].

The shear deformable sandwich FGM cylindrical shells with the porous core are considered in this present report. The shells are stiffened by shear deformable spiral FGM stiffeners. These structures have potential applications in many engineering designs, such as structures for building construction, mechanical engineering, and aerospace. An improved smeared stiffener technique is developed for shear deformable FGM stiffeners and the buckling

analysis of stiffened FGM cylindrical shells with porous cores subjected to axial compression is investigated and remarked. The adjacent equilibrium criterion and the first-order shear deformation theory (FSDT) are used to obtain the explicit expression of the critical buckling of shells. The effects of porous core, spiral FGM stiffeners, including the volume fraction index, porosity coefficient, and geometrical parameters on the axial buckling behavior of FGM cylindrical shells with porous core are investigated.

2. Sandwich FGM cylindrical shells with porous core

The considered sandwich FGM cylindrical shells with porous core in this paper are investigated with the axial compression r, the length L in the longitudinal direction, the radius R measured to the mid-plane of the shell, and the thickness h including many layers. The quasi-Cartesian coordinate system and configuration of the shell can be recognized in Fig 1. Considering that the sandwich FGM cylindrical shells with the porous core is stiffened by the spiral FGM stiffeners at the inside surface of the shell. The continuous condition of stiffener design between shell and stiffener system can be satisfied if the stiffeners are made by FGM with the selected distribution law. The material properties of shells and stiffeners are referred to Ref. [4].

Effective properties of the shell are given by [4]

$$E_{sh}(z) =$$

$$\begin{cases} E_c + E_{mc}\left(\dfrac{2z+h}{h-h_{co}}\right)^k & \text{for } -\dfrac{h}{2} \le z \le -\dfrac{h_{co}}{2}, \\[2mm] E_m\left[1 - e_0 \cos\left(\dfrac{\pi z}{h_{co}}\right)\right] & \text{for } -\dfrac{h_{co}}{2} \le z \le \dfrac{h_{co}}{2}, \\[2mm] E_c + E_{mc}\left(\dfrac{-2z+h}{h-h_{co}}\right)^k & \text{for } \dfrac{h_{co}}{2} \le z \le \dfrac{h}{2}. \end{cases} \quad (1)$$

where e_0 is porosity coefficient of the core, and $E_{mc} = E_m - E_c$.

In order to ensure the continuity between the shell and stiffeners, the effective properties of stiffeners are given by [4]

$$E_{sl} = E_c + E_{mc}\left(\frac{-2z-h}{2h_l}\right)^{k_l} \text{ for } -\frac{h}{2} - h_l \le z \le -\frac{h}{2}, (2)$$

The strain components of any point in the shell at a distance z from the mid-surface are

$$\begin{Bmatrix} \varepsilon_x \\ \varepsilon_y \\ \gamma_{xy} \end{Bmatrix} = \begin{Bmatrix} \varepsilon_x^0 \\ \varepsilon_y^0 \\ \gamma_{xy}^0 \end{Bmatrix} + z \begin{Bmatrix} \dfrac{\partial \phi_x}{\partial x} \\[2mm] \dfrac{\partial \phi_y}{\partial y} \\[2mm] \dfrac{\partial \phi_x}{\partial y} + \dfrac{\partial \phi_y}{\partial x} \end{Bmatrix},$$

$$\begin{Bmatrix} \gamma_{xz} \\ \gamma_{yz} \end{Bmatrix} = \begin{Bmatrix} \gamma_{xz}^0 \\ \gamma_{yz}^0 \end{Bmatrix}. \quad (3)$$
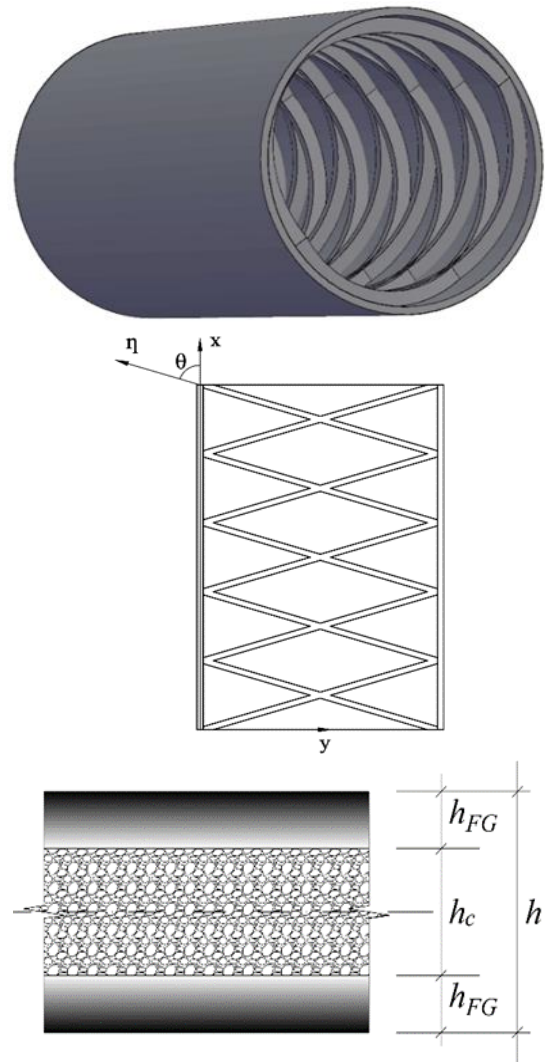

Fig. 1. Model of spiral stiffened cylindrical shells with porous core

The relations between the deformation and displacement at the mid-surface of the shell are

$$
\begin{Bmatrix} \varepsilon_x^0 \\ \varepsilon_y^0 \\ \gamma_{xy}^0 \end{Bmatrix} = \begin{Bmatrix} \dfrac{\partial u}{\partial x} \\ \dfrac{\partial v}{\partial y} - \dfrac{w}{R} \\ \dfrac{\partial u}{\partial y} + \dfrac{\partial v}{\partial x} \end{Bmatrix}, \quad \begin{Bmatrix} \gamma_{xz}^0 \\ \gamma_{yz}^0 \end{Bmatrix} = \begin{Bmatrix} \phi_x + \dfrac{\partial w}{\partial x} \\ \phi_y + \dfrac{\partial w}{\partial y} \end{Bmatrix}, \quad (4)
$$

where u, v, w are the displacement components of shells; ϕ_x and ϕ_y are the rotations of normal.

Hooke's law is applied to unstiffened shells, as

$$
\begin{Bmatrix} \sigma_x^{sh} \\ \sigma_y^{sh} \end{Bmatrix} = \frac{E}{1-v^2} \begin{bmatrix} 1 & v \\ v & 1 \end{bmatrix} \begin{Bmatrix} \varepsilon_x \\ \varepsilon_y \end{Bmatrix},
$$

$$
\begin{Bmatrix} \sigma_{xy}^{sh} \\ \sigma_{xz}^{sh} \\ \sigma_{yz}^{sh} \end{Bmatrix} = \frac{E}{2(1+v)} \begin{Bmatrix} \gamma_{xy} \\ \gamma_{xz} \\ \gamma_{yz} \end{Bmatrix}, \quad (5)
$$

and for spiral stiffeners

$$
\sigma_\eta^{sl} = E\varepsilon_\eta, \quad \sigma_{\eta z}^{sl} = \frac{E}{2(1+v)}\gamma_{\eta z}, \quad (6)
$$

where the denotes "sh" and "sl" present the shell and spiral stiffeners, respectively.

From Eq. (4), the strain components must satisfy the strain compatibility equation

$$
\frac{\partial^2 \varepsilon_x^0}{\partial y^2} + \frac{\partial^2 \varepsilon_y^0}{\partial x^2} - \frac{\partial^2 \gamma_{xy}^0}{\partial x \partial y} + \frac{1}{R}\frac{\partial^2 w}{\partial x^2} = 0. \quad (7)
$$

The internal force-strain relations are determined by integrating Hooke's law equations for the shell and for the stiffeners, applying Lekhnitskii's stiffener technique, as

$$
\begin{Bmatrix} N_x \\ N_y \\ N_{xy} \\ M_x \\ M_y \\ M_{xy} \end{Bmatrix} = \begin{bmatrix} A_{11} & A_{12} & 0 & B_{11} & B_{12} & 0 \\ A_{12} & A_{22} & 0 & B_{12} & B_{22} & 0 \\ 0 & 0 & A_{66} & 0 & 0 & B_{66} \\ B_{11} & B_{12} & 0 & D_{11} & D_{12} & 0 \\ B_{12} & B_{22} & 0 & D_{12} & D_{22} & 0 \\ 0 & 0 & B_{66} & 0 & 0 & D_{66} \end{bmatrix}
$$

$$
\times \begin{Bmatrix} \varepsilon_x^0 \\ \varepsilon_y^0 \\ \gamma_{xy}^0 \\ \dfrac{\partial \phi_x}{\partial x} \\ \dfrac{\partial \phi_y}{\partial y} \\ \dfrac{\partial \phi_x}{\partial y} + \dfrac{\partial \phi_y}{\partial x} \end{Bmatrix}, \quad (8)
$$

and the shear forces

$$
\begin{Bmatrix} Q_x \\ Q_y \end{Bmatrix} = K_s \begin{Bmatrix} H_{44}\dfrac{\partial w}{\partial x} + H_{44}\phi_x \\ H_{55}\dfrac{\partial w}{\partial y} + H_{55}\phi_y \end{Bmatrix}, \quad (9)
$$

with $K_s = 5/6$ is the shear correction factor, and

$$
A_{11} = \frac{E_1}{1-v^2} + \mu_1 2\cos^4\theta \frac{b_l}{d_l} E_1^{sl},
$$

$$
A_{12} = \frac{E_1 v}{1-v^2} + \mu_1 2\sin^2\theta\cos^2\theta \frac{b_l}{d_l} E_1^{sl},
$$

$$
A_{22} = \frac{E_1}{1-v^2} + \mu_1 2\sin^4\theta \frac{b_l}{d_l} E_1^{sl},
$$

$$
A_{66} = \frac{E_1}{2(1+v)} + \mu_1 2\sin^2\theta\cos^2\theta \frac{b_l}{d_l} E_1^{sl},
$$

$$
B_{11} = \frac{E_2}{1-v^2} + \mu_1 2\cos^4\theta \frac{b_l}{d_l} E_2^{sl},
$$

$$
B_{12} = \frac{E_2 v}{1-v^2} + \mu_1 2\sin^2\theta\cos^2\theta \frac{b_l}{d_l} E_2^{sl},
$$

$$
B_{22} = \frac{E_2}{1-v^2} + \mu_1 2\sin^4\theta \frac{b_l}{d_l} E_2^{sl},
$$

$$
B_{66} = \frac{E_2}{2(1+v)} + \mu_1 2\sin^2\theta\cos^2\theta \frac{b_l}{d_l} E_2^{sl},
$$

$$
D_{11} = \frac{E_3}{1-v^2} + \mu_1 2\cos^4\theta \frac{b_l}{d_l} E_3^{sl},
$$

$$
D_{12} = \frac{v E_3}{1-v^2} + \mu_1 2\sin^2\theta\cos^2\theta \frac{b_l}{d_l} E_3^{sl},
$$

$$
D_{22} = \frac{E_3}{1-v^2} + \mu_1 2\sin^4\theta \frac{b_l}{d_l} E_3^{sl},
$$

$$
D_{66} = \frac{E_3}{2(1+v)} + \mu_1 2\sin^2\theta\cos^2\theta \frac{b_l}{d_l} E_3^{sl},
$$

$$H_{44} = \frac{E_1}{2(1+\nu)} + \mu_1 2\sin^2\theta \frac{1}{2(1+\nu)} \frac{b_l}{d_l} E_1^{sl},$$

$$H_{55} = \frac{E_1}{2(1+\nu)} + \mu_1 2\cos^2\theta \frac{1}{2(1+\nu)} \frac{b_l}{d_l} E_1^{sl},$$

where $\mu_1 = 0$ is applied for unstiffened shells; $\mu_1 = 1$ is applied for stiffened shells, E_j, E_j^{sl} are determined as

$$E_1 = \frac{E_{mc}(h - h_{co})}{k+1}$$

$$+ E_c(h - h_{co}) + \frac{h_{co}(\pi - 2e_0)E_m}{\pi}, \quad E_2 = 0,$$

$$E_3 = \frac{E_c(h-h_{co})}{12}(h^2 + hh_{co} + h_{co}^2)$$

$$+ \frac{E_m h_{co}^3(\pi^3 - 6\pi^2 e_0 + 48e_0)}{12\pi^3} +$$

$$\frac{E_{mc}(h-h_{co})\left[\frac{k^2+3k+2}{2}h_{co}^2 + hh_{co}(k+1) + h^2 \right]}{2(k+2)(k+1)(k+3)}$$

$$E_1^{sl} = h_l E_c + \frac{h_l E_{mc}}{k_l + 1}$$

$$E_2^{sl} = -\frac{E_c(hh_l + h_l)}{2} - E_{mc}\left(\frac{h_l^2}{k_l+2} + \frac{hh_l}{2k_l+2} \right),$$

$$E_3^{sl} = \frac{E_c\left[\left(\frac{h}{2} + h_l \right)^3 - \frac{h^3}{8} \right]}{3}$$

$$+ E_{mc}\left(\frac{h_l^3}{k_l+3} + \frac{hh_l^2}{k_l+2} + \frac{h^2 h_l}{4k_l+4} \right),$$

b_l, h_l and d_l are the width, thickness and distance of the oblique stiffeners, respectively.

Eq. (8) can be oppositely rewritten by

$$\varepsilon_x^0 = A_{22}^* N_x + A_{12}^* N_y + B_{11}^* \frac{\partial\phi_x}{\partial x} + B_{12}^* \frac{\partial\phi_y}{\partial y},$$

$$\varepsilon_y^0 = A_{11}^* N_y + A_{12}^* N_x + B_{21}^* \frac{\partial\phi_x}{\partial x} + B_{22}^* \frac{\partial\phi_y}{\partial y}, \quad (10)$$

$$\gamma_{xy}^0 = N_{xy} A_{66}^* + B_{66}^*\left(\frac{\partial\phi_x}{\partial y} + \frac{\partial\phi_y}{\partial x} \right),$$

where

$$\Delta = A_{11}A_{22} - A_{12}^2, A_{11}^* = \frac{A_{11}}{\Delta}, A_{22}^* = \frac{A_{22}}{\Delta},$$

$$A_{12}^* = \frac{-A_{12}}{\Delta}, A_{66}^* = \frac{1}{A_{66}}, B_{11}^* = -A_{22}^* B_{11} - A_{12}^* B_{12},$$

$$B_{22}^* = -A_{11}^* B_{22} - A_{12}^* B_{12}, B_{12}^* = -A_{22}^* B_{12} - A_{12}^* B_{22},$$

$$B_{21}^* = -A_{11}^* B_{12} - A_{12}^* B_{11}, B_{66}^* = -\frac{B_{66}}{A_{66}},$$

Substituting Eq. (10) into Eq. (6), leads to

$$M_x = D_{11}^* \frac{\partial\phi_x}{\partial x} + D_{12}^* \frac{\partial\phi_y}{\partial y} - B_{11}^* N_x - B_{21}^* N_y,$$

$$M_y = D_{21}^* \frac{\partial\phi_x}{\partial x} + D_{22}^* \frac{\partial\phi_y}{\partial y} - B_{12}^* N_x - B_{22}^* N_y, \quad (11)$$

$$M_{xy} = -B_{66}^* N_{xy} + D_{66}^*\left(\frac{\partial\phi_x}{\partial y} + \frac{\partial\phi_y}{\partial x} \right),$$

where

$$D_{11}^* = D_{11} + B_{11}B_{11}^* + B_{12}B_{21}^*,$$

$$D_{22}^* = D_{22} + B_{12}B_{12}^* + B_{22}B_{22}^*,$$

$$D_{12}^* = D_{12} + B_{11}B_{12}^* + B_{12}B_{22}^*,$$

$$D_{21}^* = D_{12} + B_{12}B_{11}^* + B_{22}B_{21}^*,$$

$$D_{66}^* = D_{66} + B_{66}B_{66}^*.$$

The system of equilibrium equations of the shell based on FSDT is, respectively, as

$$\frac{\partial N_x}{\partial x} + \frac{\partial N_{xy}}{\partial y} = 0,$$

$$\frac{\partial N_{xy}}{\partial x} + \frac{\partial N_y}{\partial y} = 0,$$

$$\frac{\partial Q_x}{\partial x} + \frac{\partial Q_y}{\partial y} + N_x \frac{\partial^2 w}{\partial x^2}$$

$$+ 2N_{xy} \frac{\partial^2 w}{\partial x \partial y} + N_y \frac{\partial^2 w}{\partial y^2} + \frac{N_y}{R} = 0, \qquad (12)$$

$$\frac{\partial M_x}{\partial x} + \frac{\partial M_{xy}}{\partial y} - Q_x = 0,$$

$$\frac{\partial M_{xy}}{\partial x} + \frac{\partial M_y}{\partial y} - Q_y = 0,$$

The stress function can be introduced as

$$N_x = \frac{\partial^2 f}{\partial y^2}; \quad N_y = \frac{\partial^2 f}{\partial x^2}; \quad N_{xy} = \frac{\partial^2 f}{\partial x \partial y} \qquad (13)$$

Substituting Eq. (19) into compatibility

equation (7) and Eq. (11) into three end equations of (12), considering Eqs. (4) and (13), lead to

$$K_s H_{44} \frac{\partial \phi_x}{\partial x} + K_s H_{55} \frac{\partial \phi_y}{\partial y} + N_x \frac{\partial^2 w}{\partial x^2}$$

$$+ K_s H_{44} \frac{\partial^2 w}{\partial x^2} + K_s H_{55} \frac{\partial^2 w}{\partial y^2} \tag{14}$$

$$+ 2N_{xy} \frac{\partial^2 w}{\partial x \partial y} + N_y \frac{\partial^2 w}{\partial y^2} + \frac{N_y}{R} = 0,$$

$$\left(-B_{11}^* + B_{66}^* \right) \frac{\partial^3 f}{\partial x \partial y^2} - B_{21}^* \frac{\partial^3 f}{\partial x^3}$$

$$+ D_{11}^* \frac{\partial^2 \phi_x}{\partial x^2} + \left(D_{12}^* + D_{66}^* \right) \frac{\partial^2 \phi_y}{\partial x \partial y} + \tag{15}$$

$$+ D_{66}^* \frac{\partial^2 \phi_x}{\partial y^2} - K_s H_{44} \phi_x - K_s H_{44} \frac{\partial w}{\partial x} = 0,$$

$$\left(B_{66}^* - B_{22}^* \right) \frac{\partial^3 f}{\partial x^2 \partial y} - B_{12}^* \frac{\partial^3 f}{\partial y^3} + D_{22}^* \frac{\partial^2 \phi_y}{\partial y^2}$$

$$+ \left(D_{21}^* + D_{66}^* \right) \frac{\partial^2 \phi_x}{\partial x \partial y} + D_{66}^* \frac{\partial^2 \phi_y}{\partial x^2} \tag{16}$$

$$- K_s H_{55} \phi_y - K_s H_{55} \frac{\partial w}{\partial y} = 0,$$

$$A_{11}^* \frac{\partial^4 f}{\partial x^4} + \left(A_{66}^* + 2A_{12}^* \right) \frac{\partial^4 f}{\partial x^2 \partial y^2} + A_{22}^* \frac{\partial^4 f}{\partial y^4}$$

$$+ B_{21}^* \frac{\partial^3 \phi_x}{\partial x^3} + \left(B_{11}^* - B_{66}^* \right) \frac{\partial^3 \phi_x}{\partial x \partial y^2} + \frac{1}{R} \frac{\partial^2 w}{\partial x^2} \tag{17}$$

$$+ \left(B_{22}^* - B_{66}^* \right) \frac{\partial^3 \phi_y}{\partial x^2 \partial y} + B_{12}^* \frac{\partial^3 \phi_y}{\partial y^3} = 0.$$

It is assumed that equilibrium state of the shells is represented by displacement components u_0, v_0, w_0, ϕ_x^0, ϕ_y^0 and the internal forces N_x^0, N_y^0, N_{xy}^0, M_x^0, M_y^0, M_{xy}^0, Q_x^0, Q_y^0, the adjacent equilibrium can be determined by the displacement components

$$u = u_0 + u_1, \; v = v_0 + v_1, \; w = w_0 + w_1,$$

$$\phi_x = \phi_x^0 + \phi_x^1, \; \phi_y = \phi_y^0 + \phi_y^1, \tag{18}$$

and the corresponding internal forces

$$N_x = N_x^0 + N_x^1,$$

$$N_y = N_y^0 + N_y^1, \tag{19}$$

$$N_{xy} = N_{xy}^0 + N_{xy}^1,$$

$$M_x = M_x^0 + M_x^1,$$

$$M_y = M_y^0 + M_y^1, \tag{20}$$

$$M_{xy} = M_{xy}^0 + M_{xy}^1,$$

$$Q_x = Q_x^0 + Q_x^1,$$

$$Q_y = Q_y^0 + Q_y^1, \tag{21}$$

where $u_1, v_1, w_1, \phi_x^1, \phi_y^1$ and $N_{ij}^1, M_{ij}^1, Q_{ij}^1$ are the displacement and force increments, respectively.

Substituting Eqs. (19-21) into the Eq. (12) with the note that the corresponding quantities in the basic equilibrium state as well as in the neighbouring equilibrium state satisfy the equation equilibrium and the governing relations, leads to

$$\frac{\partial N_x^1}{\partial x} + \frac{\partial N_{xy}^1}{\partial y} = 0,$$

$$\frac{\partial N_{xy}^1}{\partial x} + \frac{\partial N_y^1}{\partial y} = 0,$$

$$\frac{\partial Q_x^1}{\partial x} + \frac{\partial Q_y^1}{\partial y} + N_x^0 \frac{\partial^2 w}{\partial x^2} + 2N_{xy}^0 \frac{\partial^2 w}{\partial x \partial y}$$

$$+ N_y^0 \frac{\partial^2 w}{\partial y^2} + \frac{N_y^1}{R} = 0, \tag{22}$$

$$\frac{\partial M_x^1}{\partial x} + \frac{\partial M_{xy}^1}{\partial y} - Q_x^1 = 0,$$

$$\frac{\partial M_{xy}^1}{\partial x} + \frac{\partial M_y^1}{\partial y} - Q_y^1 = 0,$$

The relations for strain increments and internal force increments are also of the form (10) and (11), performing the transformation steps as above to get Eqs. (14-17), finally get the equations

$$K_s H_{44} \frac{\partial \phi_x^1}{\partial x} + K_s H_{55} \frac{\partial \phi_y^1}{\partial y} + K_s H_{44} \frac{\partial^2 w_1}{\partial x^2}$$

$$+ K_s H_{55} \frac{\partial^2 w_1}{\partial y^2} + N_x^0 \frac{\partial^2 w_1}{\partial x^2} \tag{23}$$

$$+ 2N_{xy}^0 \frac{\partial^2 w_1}{\partial x \partial y} + N_y^0 \frac{\partial^2 w_1}{\partial y^2} + \frac{1}{R} \frac{\partial^2 f_1}{\partial x^2} = 0,$$

$$\left(B_{66}^* - B_{11}^* \right) \frac{\partial^3 f_1}{\partial x \partial y^2} - B_{21}^* \frac{\partial^3 f_1}{\partial x^3} + D_{11}^* \frac{\partial^2 \phi_x^1}{\partial x^2}$$

$$+ \left(D_{12}^* + D_{66}^* \right) \frac{\partial^2 \phi_y^1}{\partial x \partial y} + D_{66}^* \frac{\partial^2 \phi_x^1}{\partial y^2} \tag{24}$$

$$- K_s H_{44} \phi_x^1 - K_s H_{44} \frac{\partial w_1}{\partial x} = 0,$$

$$\left(B_{66}^* - B_{22}^* \right) \frac{\partial^3 f_1}{\partial x^2 \partial y} - B_{12}^* \frac{\partial^3 f_1}{\partial y^3} + D_{22}^* \frac{\partial^2 \phi_y^1}{\partial y^2}$$

$$+ \left(D_{21}^* + D_{66}^* \right) \frac{\partial^2 \phi_x^1}{\partial x \partial y} + D_{66}^* \frac{\partial^2 \phi_y^1}{\partial x^2} \tag{25}$$

$$- K_s H_{55} \phi_y^1 - K_s H_{55} \frac{\partial w_1}{\partial y} = 0,$$

$$A_{11}^* \frac{\partial^4 f_1}{\partial x^4} + \left(A_{66}^* + 2A_{12}^* \right) \frac{\partial^4 f_1}{\partial x^2 \partial y^2}$$

$$+ A_{22}^* \frac{\partial^4 f_1}{\partial y^4} + B_{21}^* \frac{\partial^3 \phi_x^1}{\partial x^3}$$

$$+ \left(B_{11}^* - B_{66}^* \right) \frac{\partial^3 \phi_x^1}{\partial x \partial y^2} + \left(B_{22}^* - B_{66}^* \right) \frac{\partial^3 \phi_y^1}{\partial x^2 \partial y} \tag{26}$$

$$+ B_{12}^* \frac{\partial^3 \phi_y^1}{\partial y^3} + \frac{1}{R} \frac{\partial^2 w_1}{\partial x^2} = 0.$$

Consider the state before instability as the membrane state of simply supported cylindrical shells, where the axial force and moment components are determined by

$$N_x^0 = -rh,$$

$$N_y^0 = N_{xy}^0 = 0,$$

$$M_x^0 = M_y^0 = M_{xy}^0 = 0, \tag{27}$$

$$Q_x^0 = Q_y^0 = 0.$$

The boundary condition (27) considered in this case corresponds to increments is in the form

$$w_1 = M_x^1 = N_x^1 = N_{xy}^1 = 0, \text{ at } x = 0; L. \tag{28}$$

Boundary condition (28) can be satisfied if the solution is chosen by

$$w_1 = \sum_m \sum_n W_{mn} \sin \frac{m\pi x}{L} \sin \frac{ny}{R},$$

$$\phi_{1x} = \sum_m \sum_n \Phi_x^{mn} \cos \frac{m\pi x}{L} \sin \frac{ny}{R}, \tag{29}$$

$$\phi_{1y} = \sum_m \sum_n \Phi_y^{mn} \sin \frac{m\pi x}{L} \cos \frac{ny}{R},$$

where m and n are the half waves in x and y directions.

3. Solution procedure

Substituting Eq. (29) into Eq. (26), solving the resulting equation to get the stress function, as

$$f_1 = \sum_m \sum_n f_{mn} \sin \frac{m\pi x}{L} \sin \frac{ny}{R}, \tag{30}$$

with

$$\alpha = \frac{m\pi}{L}, \quad \beta = \frac{n}{R}, \quad f_{mn} = \frac{\alpha^2}{AR} W + \frac{B}{A} \Phi_x + \frac{C}{A} \Phi_y,$$

$$A = \alpha^4 A_{11}^* + \beta^2 \left(A_{66}^* + 2A_{12}^* \right) \alpha^2 + \beta^4 A_{22}^*,$$

$$B = -B_{21}^* \alpha^3 - \alpha\beta^2 \left(B_{11}^* - B_{66}^* \right),$$

$$C = -B_{12}^* \beta^3 - \alpha^2 \beta \left(B_{22}^* - B_{66}^* \right).$$

Putting expressions (29) and (30) into Eqs. (23-25), leads to

$$\sum_m \sum_n \left\{ \begin{bmatrix} c_{11}\Phi_x^{mn} + c_{12}\Phi_y^{mn} \\ + \left(c_{13} + \alpha^2 rh \right) W_{mn} \end{bmatrix} \\ \times \sin \frac{m\pi x}{L} \sin \frac{ny}{R} \right\} = 0 \tag{31}$$

$$\sum_m \sum_n \left\{ \begin{bmatrix} a_{11}\Phi_x^{mn} + a_{12}\Phi_y^{mn} \\ + a_{13} W_{mn} \end{bmatrix} \\ \times \cos \frac{m\pi x}{L} \sin \frac{ny}{R} \right\} = 0, \tag{32}$$

$$\sum_m \sum_n \left\{ \begin{bmatrix} b_{11}\Phi_x^{mn} + b_{12}\Phi_y^{mn} + b_{13} W_{mn} \end{bmatrix} \\ \times \sin \frac{m\pi x}{L} \cos \frac{ny}{R} \right\} = 0, \tag{33}$$

with

$$a_{11} = -\alpha^2 D_{11}^* - \beta^2 D_{66}^* - H_{44} K_s$$
$$+ \frac{\left[\alpha^3 B_{21}^* + \left(B_{11}^* - B_{66}^*\right)\beta^2\alpha\right]B}{A}$$

$$a_{12} = -\left(D_{66}^* + D_{12}^*\right)\beta\alpha$$
$$+ \frac{\left[\alpha^3 B_{21}^* + \left(B_{11}^* - B_{66}^*\right)\beta^2\alpha\right]C}{A}$$

$$a_{13} = \frac{\left[\alpha^3 B_{21}^* + \left(B_{11}^* - B_{66}^*\right)\beta^2\alpha\right]\alpha^2}{AR} - K_s H_{44}\alpha$$

$$b_{12} = -\alpha^2 D_{66}^* - \beta^2 D_{22}^* - H_{55} K_s$$
$$+ \frac{\left[\beta^3 B_{12}^* + \left(B_{22}^* - B_{66}^*\right)\alpha^2\beta\right]C}{A}$$

$$b_{11} = -\left(D_{66}^* + D_{21}^*\right)\beta\alpha$$
$$+ \frac{\left[\beta^3 B_{12}^* + \left(B_{22}^* - B_{66}^*\right)\alpha^2\beta\right]B}{A}$$

$$b_{13} = \frac{\left[\beta^3 B_{12}^* + \left(B_{22}^* - B_{66}^*\right)\alpha^2\beta\right]\alpha^2}{AR} - K_s H_{55}\beta$$

$$c_{11} = -\frac{B\alpha^2}{AR} - H_{44} K_s\alpha, c_{12} = -K_s H_{55}\beta - \frac{\alpha^2 C}{AR},$$

$$c_{13} = -K_s\left(H_{44}\alpha^2 + H_{55}\beta^2\right) - \frac{\alpha^4}{R^2 A}$$

Eqs. (31), (32) and (33) are satisfied vs. x, y, i.e.

$$c_{11}\Phi_x^{mn} + c_{12}\Phi_y^{mn} + \left(c_{13} + \alpha^2 rh\right)W_{mn} = 0 \qquad (34)$$

$$a_{11}\Phi_x^{mn} + a_{12}\Phi_y^{mn} + a_{13}W_{mn} = 0 \qquad (35)$$

$$b_{11}\Phi_x^{mn} + b_{12}\Phi_y^{mn} + b_{13}W_{mn} = 0 \qquad (36)$$

From Eqs. (33) and (34), the relations between Φ_x^{mn}, Φ_y^{mn} and W_{mn} are obtained as

$$\Phi_x^{mn} = \frac{a_{12}b_{13} - a_{13}b_{12}}{a_{11}b_{12} - a_{12}b_{11}}W_{mn} \qquad (37)$$

$$\Phi_y^{mn} = \frac{a_{13}b_{11} - a_{11}b_{13}}{a_{11}b_{12} - a_{12}b_{11}}W_{mn} \qquad (38)$$

Substituting Eqs. (35) and (36) into Eq. (32), neglecting the solution $W_{mn} = 0$, the critical buckling load of shell can be determined as

$$r_{cr} = -\big(a_{11}b_{12}c_{13} - a_{11}b_{13}c_{12}$$
$$- a_{12}b_{11}c_{13} + a_{12}b_{13}c_{11} + a_{13}b_{11}c_{12} \qquad (39)$$
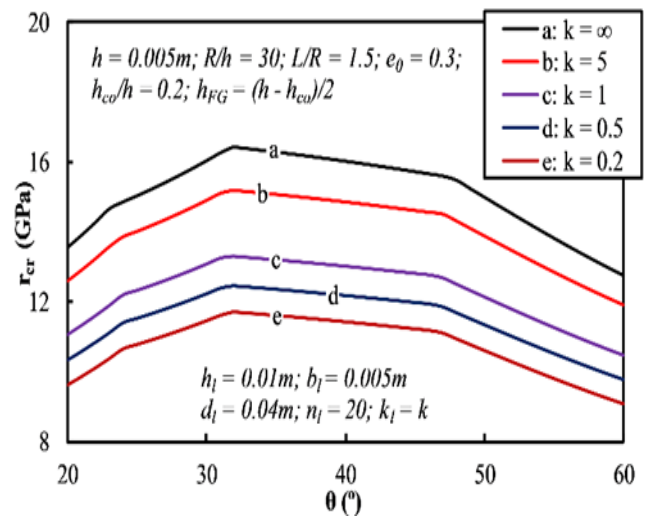$$- a_{13}b_{12}c_{11}\big)/\left[\left(a_{11}b_{12} - a_{12}b_{11}\right)\alpha^2 h\right]$$

4. Validation and numerical investigations

Table 1. Comparisons of critical buckling compression r_{cr} (in kN) for perfect FGM cylindrical shells ($R/h = 40$, $L^2/Rh = 500$)
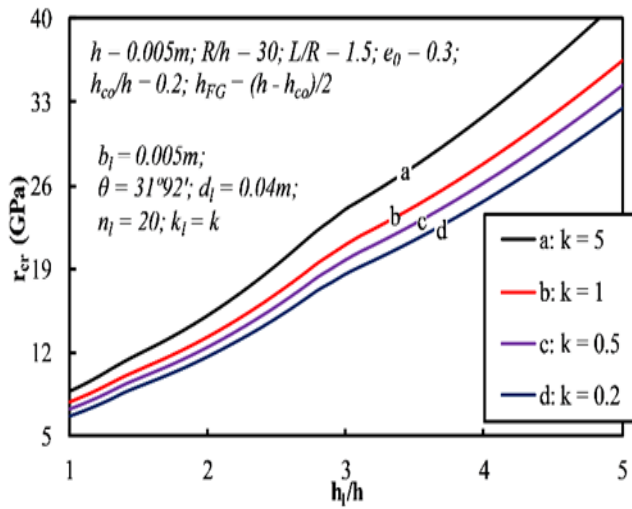
	Shen [2]	Present
$k = 0$	118516.6(5;5)	126548.22(5;5)
$k = 0.2$	110800.8(5;5)	117025.15(5;5)
$k = 1$	96918.5(5;5)	99942.76(5;5)
$k = 2$	90853.3(5;5)	92722.28(5;5)
$k = 5$	84853.4(5;5)	86620.73(5;5)

To validate the present approach, the critical buckling loads of the present study with those of Shen [2] for FGM cylindrical shells in Table 1. As can be observed, good agreements are obtained.
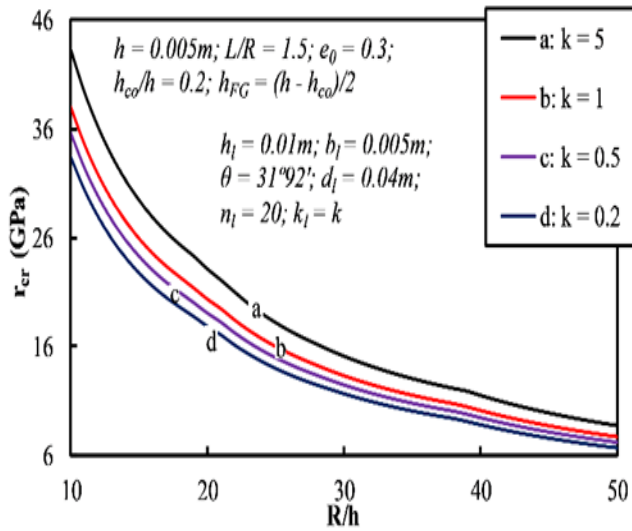
Fig. 2 presents the effects of stiffener angle on the critical buckling load of shells. Clearly, the critical buckling loads of shells increase when the stiffener angle increases, and it decreases after a maximum point. The most effective stiffener angle in these investigations was achieved in the range of 34 degrees.
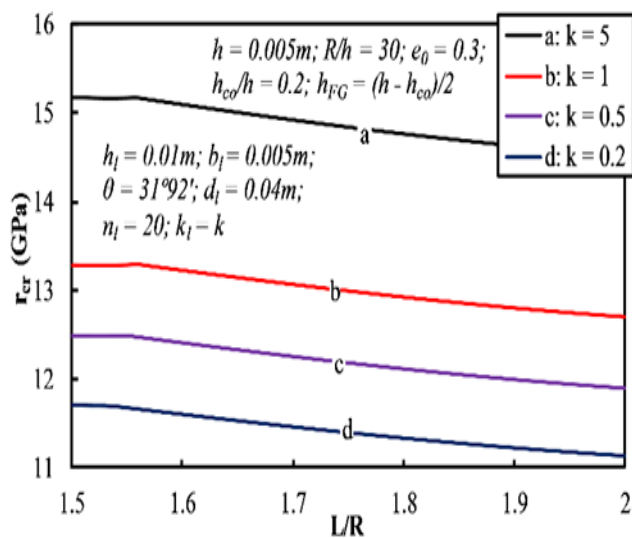

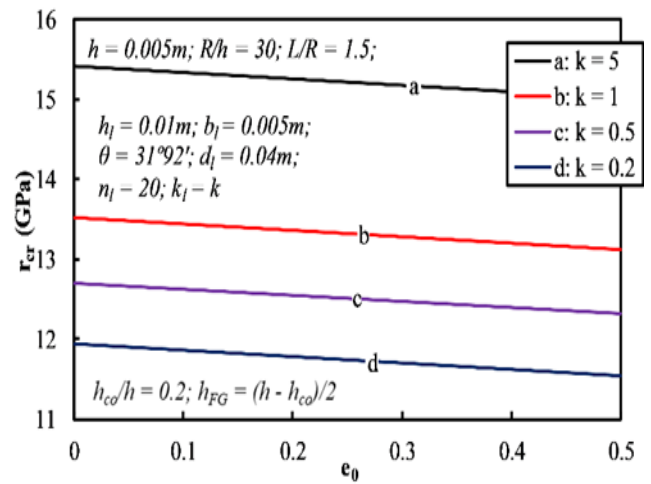**Fig. 2.** Effects of stiffener angle on the critical buckling load of shells

Fig. 3. Effects of height of stiffeners on the critical buckling load of shells
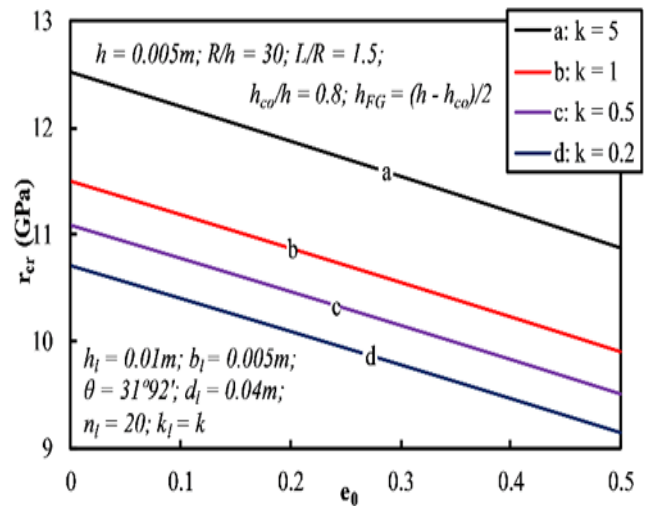

Fig. 4. Effects of R/h ratio on the critical buckling load of shells

Fig. 5. Effects of L/R ratio on the critical buckling load of shells

Fig. 6. Effects of porosity coefficients e_0 on the critical buckling load of shells ($h_{co}/h = 0.2$)

Fig. 7. Effects of porosity coefficients e_0 on the critical buckling load of shells ($h_{co}/h = 0.8$)

The height of stiffeners also greatly affects the critical buckling load of the shell. As can be seen in Fig. 3, the critical buckling load of shells greatly increases when the height of the stiffener increases. It is obvious that when the stiffener height is large, the eccentricity of the stiffener is also large, leading to a larger total stiffnesses of stiffened shells.

The effects of the R/h ratio on the critical buckling of shells are presented in Fig. 4. Clearly, the critical buckling load decreases when the R/h ratio increases. In other words, the thinner the shell, the lower the load-carrying capacity of the shell.

Similarly, the strong effects of the L/R ratio

on the critical buckling load of shells are presented in Fig. 5. The decreasing trend of the critical buckling load as L/R increases is shown at all values of the volume fraction indexes. In other words, the longer the shell, the lower the load-carrying capacity of the shell. Effects of porosity coefficients e_0 on the critical buckling load of shells are presented in Figs. 6 and 7 with $h_{co}/h = 0.2$ and $h_{co}/h = 0.8$, respectively. With small value of h_{co}/h in Fig. 6, the porosity coefficient has a small influence on the critical buckling load of the shell. Oppositely, the large effects of porosity coefficients e_0 on the critical buckling load of shells can be observed in Fig. 7 with the large value of h_{co}/h.

5. Conclusion

Based on the FSDT, the improved smeared stiffeners technique for spiral stiffeners, and the adjacent equilibrium criterion, the closed-form of the critical buckling load of stiffened sandwich FGM cylindrical shell with porous core under axial compression is presented in this paper. The numerical results present the strong effects of stiffeners, geometrical and material properties of shells, and the light effects of porosity coefficients on the critical buckling load of shells.

Acknowledgments

References

[1] H. Huang, Q. Han. (2009). Nonlinear elastic buckling and postbuckling of axially compressed functionally graded cylindrical shells. *Int J Mech Sci*, 51(7): 500-507.

[2] H.S. Shen. (2009). Postbuckling of shear deformable FGM cylindrical shells surrounded by an elastic medium. *Int J Mech Sci,* 51(5), 372-383.

[3] Sofiyev AH. (2010). Buckling analysis of FGM circular shells under combined loads and resting on the Pasternak type elastic foundation. *Mech Res Commun* 37(6): 539–544.

[4] V.H. Nam, N.T. Trung, L.K. Hoa. (2019). Buckling and postbuckling of porous cylindrical shells with functionally graded composite coating under torsion in thermal environment. *Thin Wall Struct*, 144, 106253.

[5] N.T. Phuong, D.T. Luan, V.H. Nam, P.T. Hieu. (2019). Nonlinear approach on torsional buckling and postbuckling of functionally graded cylindrical shells reinforced by orthogonal and spiral stiffeners in thermal environment. *Proc Inst Mech Eng C: J Mech Engin Sci,* 233(6), 2091–2106.

[6] V.H. Nam, N.T. Phuong, N.T. Trung. (2019). Nonlinear buckling and postbuckling of sandwich FGM cylindrical shells reinforced by spiral stiffeners under torsion loads in thermal environment. *Acta Mech*, 230, 3183–3204.

[7] V.H. Nam, N.T. Phuong, C.V. Doan and N.T. Trung. (2019). Nonlinear Thermo-Mechanical Stability Analysis of Eccentrically Spiral Stiffened Sandwich Functionally Graded Cylindrical Shells Subjected to External Pressure. *Int J Appl Mech,* 11(05), 1950045.

[8] N.T. Phuong, V.H. Nam, N.T. Trung, V.M. Duc, P.V. Phong. (2019). Nonlinear stability of sandwich functionally graded cylindrical shells with stiffeners under axial compression in thermal environment. *Int J Struct Stab Dyn*, 19(07), 1950073.

[9] L.K. Hoa, V.T. Hung, P.H. Quan, V.H. Nam. (2019). Nonlinear buckling and postbuckling of spiral stiffened FG-GPLRC cylindrical shells subjected to torsional loads. *J Sci Trans Technol*, 1(1), 26-35.

[10] H. Babaei, M. Jabbari, M.R. Eslami (2021). The Effect of Porosity on Elastic Stability of Toroidal Shell Segments Made of Saturated Porous Functionally Graded Materials. *J Pressure Vessel Technol*, 143(3), 031501.